

Solitons in strongly driven discrete nonlinear Schrödinger-type models

Josselin Garnier^{1, y}, Fatkhulla Kh. Abdullaev², and Mario Salerno³

¹ Laboratoire de Probabilités et Modèles Aléatoires & Laboratoire Jacques-Louis Lions,
Université Paris VII, 2 Place Jussieu, 75251 Paris Cedex 5, France

² Physical-Technical Institute of the Uzbekistan Academy of Sciences,
700084, Tashkent-84, G. Mavlyanov str., 2-b, Uzbekistan

³ Dipartimento di Fisica "E.R. Caianiello",
Università di Salerno, 84081 Baronissi (SA), Italy

Abstract

Discrete solitons in the Ablowitz-Ladik (AL) and discrete nonlinear Schrödinger (DNLS) equations with damping and strong rapid drive are investigated. The averaged equations have the form of the parametric AL and DNLS equations. A new type of parametric bright discrete soliton and cnoidal waves are found and the stability properties are analyzed. The analytical predictions of the perturbed inverse scattering transform are confirmed by the numerical simulations of the AL and DNLS equations with rapidly varying drive and damping.

PACS numbers: 02.30.Jr, 05.45.Yv, 03.75.Lm, 42.65.Tg

^y Corresponding author (garnier@math.jussieu.fr)

I. INTRODUCTION

Recently the problem of dynamics of nonlinear lattices under strong and rapid modulations of parameters has attracted a lot of attention. Two systems have been analyzed. The first one is the diffraction-managed array of optical waveguides, with diffraction varying periodically along the beam propagation [1]. The model is described by the discrete nonlinear Schrödinger (DNSL) equation with rapidly and strongly varying in time tunnel-coupling between sites coefficient $c(t)$:

$$iu_{nt} + \frac{1}{c(t)}(u_{n+1} + u_{n-1}) + 2j_n u_n^2 = 0; \quad (1)$$

where 1. The analysis exhibits the existence of a new type of discrete spatial optical solitons with beam width and peak amplitude evolving periodically during propagation.

The second system is the Bose-Einstein condensate in a periodic (in space) potential with a varying (in time) scattering length. In the tight-binding approximation this system is described by the DNLS equation [2] with strongly and rapidly varying in time nonlinearity coefficient $\gamma(t)$:

$$iu_{nt} + (u_{n+1} + u_{n-1}) + \frac{1}{\gamma(t)}j_n u_n^2 = 0; \quad (2)$$

It was shown that this system supports nonlinearity-managed discrete solitons [3]. In a more general context it is of interest to investigate the influence of rapid perturbations on the dynamics of discrete solitons in nonlinear lattices. The case of strongly and rapidly varying external drivers is particularly important for applications. This problem is encountered both in the study of the dynamics of a magnetic flux quantum in an array of long Josephson junctions with varying ac current [4] and in the evolution of an optical field in a nonlinear chain of resonators or microcavities in presence of pumping [5, 6, 7, 8].

In this paper we consider the influence of a rapid strong drive on discrete bright solitons and cnoidal waves of the Ablowitz-Ladik (AL) and the DNLS equations with damping. Although the AL system has scarce physical applications it has many advantages from the analytical point of view such as the complete integrability of the unperturbed system, existence of moving discrete solitons etc. In some regions of the parameter space, the DNLS equation can be described as a perturbation of the AL model, a feature that we shall take advantage of in the following. The dynamics of discrete solitons in AL and DNLS equations under the influence of damping and slowly varying driving field has been studied in Refs. [9, 10].

Recently the influence of parametric drivers on the stability of strongly localized modes of the DNLS equation near the anti-continuum limit has been investigated in [11]. The stability of solitons in the continuous parametrically driven NLS equation has been studied in [12, 13]. Here we address a general discrete nonlinear system with a strong rapid drive modeled by the following equation:

$$iu_{nt} + [u_{n+1} + u_{n-1} - (2 + \gamma)u_n] + j_n f\left[\left(1 - \frac{\gamma}{2}\right)(u_{n+1} + u_{n-1}) + 2u_n\right] = \frac{1}{\tau} f\left(\frac{t}{\tau}\right) i u_n; \quad (3)$$

where f is a zero-mean periodic function with period 1 that describes the rapid drive, and the small parameter τ is the period of the drive. Here the parameter $\gamma \geq 0$ denotes the damping term, γ is the propagation constant in optics (chemical potential in BECs), and the parameter $\gamma \in [0; 1]$ characterizes the type of nonlinearity. For $\gamma = 0$ the nonlinearity is of intersite type as in the AL model while for $\gamma = 1$ we have the onsite nonlinearity of the DNLS equation. In absence of strong rapid drive and damping Eq. (3) coincides with the Salerno model [14] which interpolates between the AL model and the DNLS model. We show that by averaging out the fast time scale one can reduce Eq. (3), for particular choices of parameters, to the parametrically driven AL and DNLS equations with damping. The existence of parametric discrete bright solitons and cnoidal waves of these equations is then investigated and the stability properties is analyzed both analytically and numerically. We find that the analytical predictions obtained from the averaged equations by means of a perturbation scheme based on the inverse scattering method are in good agreement with direct numerical simulations of the problem with rapidly varying drive and damping.

Finally, we remark that the physical systems where parametric discrete solitons of the type considered in this paper can be realized are chains of linearly coupled nonlinear microcavities [15] and nonlinear waveguide arrays with dielectric mirror at the ends, driven by an external time-dependent field [7, 8]. In this case the equation describing the discrete cavity solitons has the form of the parametric DNLS

$$iu_{nt} + \delta u_n + i \gamma u_n + j_n f u_n + C(u_{n+1} + u_{n-1} - 2u_n) = F_n(t); \quad (4)$$

where δ is the detuning from the linear resonance parameter, γ is the effective damping parameter, C is the effective coupling between adjacent waveguides, $F_n(t)$ is the input field in the n -th waveguide. Injecting a homogeneous in space and rapidly varying in time field, we can generate discrete parametric soliton in this system.

The paper is organized as follows. In Section II we derive the averaged DNLS-type equation for the strongly and rapidly varying external drive model. In Section III we analyze the solitons in a damped AL system with parametric drive. We use the perturbation theory based on the Inverse Scattering Transform (IST) and study the stability region of parametric discrete solitons. Periodic solutions of the damped AL equation with parametric drive are also found in this section. The discrete soliton dynamics in parametrically driven DNLS is investigated in Section IV.

II. AVERAGING

We look for the solution of Eq. (3) in the form

$$u_n(t) = u_n^{(0)}(t; \frac{t}{\mu}) + \epsilon u_n^{(1)}(t; \frac{t}{\mu}) + \dots \quad (5)$$

where $u_n^{(0)}, u_n^{(1)}, \dots$ are periodic in the argument $t = t/\mu$. We substitute this ansatz into Eq. (3) and collect the terms with the same powers of ϵ . We obtain the hierarchy of equations:

$$\begin{aligned} i u_n^{(0)} &= f(\phi_n) \\ i u_n^{(0)} + [u_{n+1}^{(0)} + u_{n-1}^{(0)} - (2 + \epsilon) u_n^{(0)}] + \epsilon u_n^{(0)2} [(1 - \epsilon) (u_{n+1}^{(0)} + u_{n-1}^{(0)}) + 2 u_n^{(0)}] &= -i u_n^{(0)} - i u_n^{(1)} \end{aligned}$$

The first equation imposes the form of the leading-order term

$$u_n^{(0)}(t; \frac{t}{\mu}) = i F(\phi_n) + a_n(t);$$

where $F(\phi) = \int_0^R f(s) ds$ is the antiderivative of f and a_n depends only on the slow variable t . The second equation is the compatibility equation for the existence of the expansion (5). By integrating over a period in ϕ , we obtain:

$$\begin{aligned} i a_{n,t} + [a_{n+1} + a_{n-1} - (2 + \epsilon) a_n] + (1 - \epsilon) \epsilon a_n - i F(\phi_n)^2 (a_{n+1} + a_{n-1} - 2 i F(\phi_n)) \\ + 2 \epsilon a_n - i F(\phi_n)^2 (a_n - i F(\phi_n)) = -i a_n \end{aligned}$$

which gives

$$\begin{aligned} i a_{n,t} + [a_{n+1} + a_{n-1} - (2 + \epsilon) a_n] + \epsilon a_n^2 [(1 - \epsilon) (a_{n+1} + a_{n-1}) + 2 a_n] \\ = -i a_n + \overline{a_n} - \frac{\epsilon}{2} [(1 - \epsilon) (a_{n+1} + a_{n-1}) + 2 (1 + \epsilon) a_n]; \end{aligned} \quad (6)$$

where $\epsilon = 2\hbar F^2 i$.

Thus, the averaging method applied to Eq. (3) leads to a parametrically driven nonlinear lattice equation which reduces to the Salerno model [14] in absence of perturbations. It is possible to consider a random forcing instead than a periodic one. More precisely, we get the same result if the source $f(t)$ is a colored noise with coherence time of order one. However, the power spectral density of the source should vanish at zero-frequency. Otherwise it would appear a phase diffusion and this would destroy the stability of the stationary solution that we will introduce next.

We introduce the rescaled time $T = t(1 + \frac{1}{2})$ and the rescaled function $A_n = \frac{p}{1 + \frac{1}{2}}$. The averaged equation for the function $A_n(T)$ has the form

$$iA_{nT} + [A_{n+1} + A_{n-1} - (2 + \frac{1}{2})A_n] + \frac{1}{2}A_n^2(A_{n+1} + A_{n-1}) = R_n; \quad (7)$$

where

$$= \frac{1}{1 + \frac{1}{2}}; \quad = \frac{1}{1 + \frac{1}{2}}; \quad = \frac{1}{1 + \frac{1}{2}};$$

and the term in the right-hand side is given by

$$R_n = iA_n + \overline{A_n} + \frac{1}{2}A_n^2(A_{n+1} + A_{n-1} - 2A_n); \quad (8)$$

The left hand side of (7) is the Ablowitz-Ladik (AL) equation, that is completely integrable. The right-hand side can be seen as a perturbation of this system. We shall use the perturbed Inverse Scattering Transform (IST) to study the evolution dynamics of AL solitons driven by the perturbation R_n .

III. THE DAMPED AL SYSTEM WITH PARAMETRIC DRIVE

We consider in this section the case $\gamma = 0$, that is the AL model with damping and rapid drive. Therefore, we consider the perturbed AL equation (7) with the perturbation

$$R_n = iA_n + \overline{A_n}; \quad (9)$$

A. Perturbed Inverse Scattering Transform

We assume that the damping parameter and the parametric drive parameter are small (but γ can be of order one). Therefore, γ and ϵ are small, and, following [16, 17, 18], the

evolution equations for the soliton parameters in the adiabatic approximation have the form

$$\begin{aligned}
 x_T &= 2 \frac{\sinh}{\cosh} \sin + \frac{\sinh}{\cosh} \sum_{n=-1}^{\infty} \frac{(n-x) \cosh(n-x) \operatorname{Im}(r)}{\cosh(n+1-x) \cosh(n-1-x)}; \\
 T &= \sinh \sum_{n=-1}^{\infty} \frac{\cosh(n-x) \operatorname{Im}(r)}{\cosh(n+1-x) \cosh(n-1-x)}; \\
 T &= \sinh \sum_{n=-1}^{\infty} \frac{\sinh(n-x) \operatorname{Re}(r)}{\cosh(n+1-x) \cosh(n-1-x)}; \\
 T &= 2 \cosh \cos + 2 \frac{\sinh}{\cosh} \sin^2 + \sinh \sum_{n=-1}^{\infty} \frac{(n-x) \sinh(n-x) \operatorname{Re}(r)}{\cosh(n+1-x) \cosh(n-1-x)} \\
 &\quad + \cosh \sum_{n=-1}^{\infty} \frac{\cosh(n-x) \operatorname{Re}(r)}{\cosh(n+1-x) \cosh(n-1-x)} \\
 &\quad + \frac{\sinh}{\cosh} \sum_{n=-1}^{\infty} \frac{(n-x) \cosh(n-x) \operatorname{Im}(r)}{\cosh(n+1-x) \cosh(n-1-x)};
 \end{aligned}$$

where $r_n = R_n \exp(i(n-x) - i)$. Using standard analytical tools (Poisson summation formula and residue theorem), we can compute the right-hand sides of these equations. The equation for T takes the form:

$$T = P^{(1)} + G^{(1)} \quad (10)$$

where

$$\begin{aligned}
 P^{(1)} &= \sinh^2 \sum_{s=-1}^{\infty} I(2 + 2s) \sin(2sx + 2); \\
 G^{(1)} &= 2 \tanh
 \end{aligned}$$

with

$$I(a) = \frac{2 \sin a}{\sinh(2) \sinh(\frac{a}{2})};$$

The equation for T has the form:

$$T = P^{(1)} + G^{(1)} \quad (11)$$

where

$$\begin{aligned}
 P^{(1)} &= \sinh^2 \sum_{s=-1}^{\infty} K(2 + 2s) \sin(2sx + 2); \\
 G^{(1)} &= 0;
 \end{aligned}$$

with

$$K(a) = \frac{2 \sin^2(a=2)}{\sinh^2 \sinh(\frac{a}{2})} ;$$

The equation for the soliton center x has the form :

$$x_T = 2 \frac{\sinh}{\cosh} \sin + P^{(x)} + G^{(x)} \quad (12)$$

where

$$P^{(x)} = \frac{\sinh^2}{\cosh} \sum_{s=1}^X J(2 + 2s) \cos(2sx + 2) ;$$

$$G^{(x)} = \frac{\sinh^2}{\cosh} (x) ;$$

with $J(a) = I^0(a)$ and

$$(x) = \sum_{n=1}^X \frac{(n-x)}{\cosh((n+1-x)) \cosh((n-1-x))} = \frac{4}{\sinh(2)} \sum_{s=1}^X \frac{\sin(2sx)}{\sinh(\frac{2s}{2})} ;$$

Finally, the equation for the soliton phase has the form :

$$x_T = 2 \cosh \cos + 2 \frac{\sinh}{\cosh} \sin + 2 + P^{(x)} + G^{(x)} \quad (13)$$

where

$$P^{(x)} = \sinh \sum_{s=1}^X L(2 + 2s) \cos(+ s + 2 + 2sx)$$

$$+ \sinh \sum_{s=1}^X K^0(2 + 2s) \sin(2sx + 2)$$

$$+ \sinh \sum_{s=1}^X K(2 + 2s) \cos(2sx + 2)$$

$$+ \frac{\sinh^2}{2} \sum_{s=1}^X I^0(2 + 2s) \sin(2sx + 2) ;$$

$$G^{(x)} = \frac{\sinh^2}{\cosh} (x) ;$$

with

$$L(a) = \frac{2 \sin(a=2)}{\sinh \sinh(\frac{a}{2})} ;$$

B. Parametrically driven AL solitons

The system (10-13) has two fixed points if $\epsilon < 1$ (which is equivalent to $\epsilon < 1$) and $\epsilon + \gamma > 0$ (which is equivalent to $\epsilon + \gamma > 0$):

$$\phi = 0; \quad \sin(2\theta) = -\frac{\epsilon}{2}; \quad \cos(2\theta) = \frac{1 - \frac{\epsilon^2}{4}}{2}; \quad (14)$$

$$\theta = \text{arccosh} \left(1 + \frac{\epsilon}{2} + \frac{\epsilon^2}{2} \cos(2\theta) \right); \quad (15)$$

In fact, the second point (with subscript 2) exists only if $\epsilon + \cos(2\theta) > 0$. The center of the soliton can be arbitrary. Note that these values correspond to a fixed point of the equation (7). The soliton is of the form

$$A_n(T) = \frac{\sinh}{\cosh[(n-x)]} e^{i\theta};$$

We can investigate the linear stability of these solutions. The linearization of the nonlinear system (10-13) around the parameters of the stationary solitons gives the linear system

$$\dot{x}_1 = 2 \sinh^2(\theta) \cos(2\theta) x_1 - 4 \tanh(\theta) \cos(2\theta) x_1; \quad (16)$$

$$\dot{x}_2 = 2 x_1; \quad (17)$$

$$\dot{x}_3 = 2 \sinh(\theta) x_1 - 2 x_1; \quad (18)$$

$$\begin{aligned} \dot{x}_{1T} = 2 \frac{\sinh}{\cosh} x_1 - \frac{\sinh^2}{3^2 \sinh(2\theta)} \cos(2\theta) x_1 \\ - \frac{\sinh^2}{\cosh^2(\theta)} (x_2) x_1 - \frac{\sinh(2\theta) \sinh^2}{2} (x_3) x_1; \end{aligned} \quad (19)$$

The equation for x_1 is decoupled from the other ones. The three eigenvalues for the 3×3 system for $(x_1; x_2; x_3)$ are

$$\begin{aligned} \lambda^{(1)} &= 2; \\ \lambda^{(2)} &= \frac{1}{2} + \frac{p}{2} \frac{8 \sinh(\theta) \tanh(\theta) \cos(2\theta)}{3^2 \sinh(2\theta)}; \\ \lambda^{(3)} &= \frac{1}{2} - \frac{p}{2} \frac{8 \sinh(\theta) \tanh(\theta) \cos(2\theta)}{3^2 \sinh(2\theta)}; \end{aligned}$$

The fixed point is stable if the real parts of the eigenvalues are nonpositive. This shows that the fixed point labeled 2 is not stable, since $\lambda^{(2)} > 0$, while the fixed point labeled + is stable.

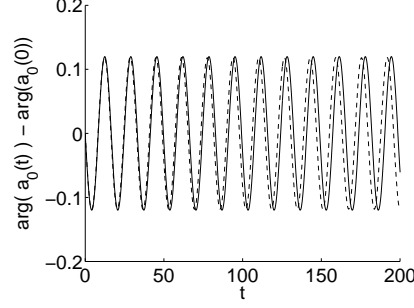


FIG. 1: Here $\gamma = 0$, $\beta = 1$, $\epsilon = 0.022$, and $\delta = 0$ (i.e. $\epsilon = 0.0218$ and $\delta = 0$). The initial condition is a soliton with $\phi = \phi_+$, $x_+ = 0$, $\dot{\phi} = 0$, and $\dot{x}_+ = \phi_+ + 0.02$ ($\phi_+ = 0.948$). We plot the solution phase obtained from the numerical integration of Eq. (6) (dashed line) and compare with the theoretical oscillation obtained from (16-18) (solid line). The theoretical oscillation period (in the t -variable) is $2\pi = 2\pi/(1 + \epsilon/2) = 16.6$.

In absence of damping $\gamma = 0$ (which is equivalent to $\delta = 0$), the soliton parameters and (amplitude and phase) oscillate with the frequency (in the T -variable)

$$\omega_+ = \frac{\epsilon}{8 \sinh \phi_+ \tanh \phi_+} \quad (20)$$

while the parameter (velocity) is constant. This means that the stationary soliton is stable. This also shows that stable slowly moving breathers can propagate in the presence of parametric drive.

We have performed numerical simulations of Eq. (6) to confirm these predictions. In Fig. 1 we consider a perturbation of the initial amplitude. The periodic oscillations of the soliton parameters have the predicted period (20). In Fig. 2 we consider a soliton with a positive velocity. As predicted by the theory, this soliton can propagate in a stable way.

In presence of damping the soliton parameters and oscillate with the frequency

$$\omega_+ = \frac{\epsilon}{8 \frac{\epsilon^2}{2} \sinh \phi_+ \tanh \phi_+ \frac{\epsilon^2}{2}} \quad (21)$$

These oscillations decay exponentially with the rate $\frac{\epsilon}{2}$. Besides, comparing (20) and (21) shows that the damping enhances the oscillation period. The soliton parameter decays exponentially at the rate 2ϵ . Therefore, the stationary soliton is very stable. However, the propagation of moving solitons is not supported, as the soliton velocity decays exponentially to 0. If we denote by ϕ_0 the initial value of the parameter ϕ , then the input soliton converges

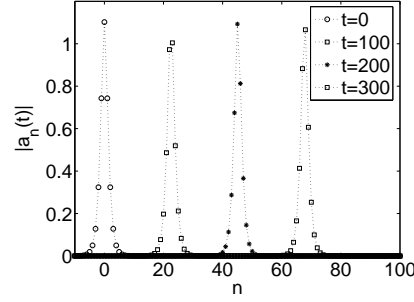


FIG. 2: Here $\beta = 0$, $\gamma = 1$, $\alpha = 0.022$, $\delta = 0$. The initial condition is a soliton with $\phi = \pi$, $x_+ = 0$, $\eta = 0.1$, and $\theta = \pi$. We plot the soliton profiles $|a_n(t)|$ at different times, which exhibits the stable propagation of the moving soliton.

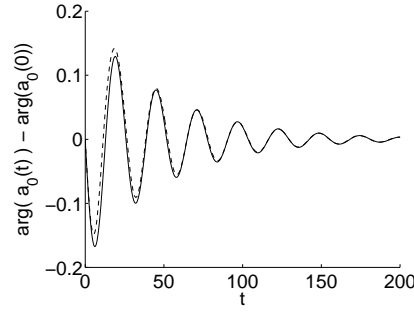


FIG. 3: Here $\beta = 0$, $\gamma = 1$, $\alpha = 0.022$, $\delta = 0.02$. The initial condition is a soliton with $\phi = \pi$, $x_+ = 0$, $\eta = 0$, and $\theta = \pi + 0.02$ ($\phi_+ = 0.942$). We plot the solution phase obtained from the numerical integration of Eq. (6) (dashed line). The observed oscillations and damping are correctly predicted by the model (16-18) (solid line). The period is $2\pi\omega_+ = (1 + \eta^2) = 25.9$ and the exponential decay rate is $\gamma = 0.02$ (solid line).

to the stationary form

$$A_n = \frac{\sinh \frac{\pi}{2}}{\cosh \left[\frac{\pi}{2} (n - x_+ - x_F) \right]} e^{i \frac{\pi}{2}}$$

with

$$x_F = \frac{\sinh \frac{\pi}{2} \sin \theta_0}{\pi} : \quad (22)$$

In Fig. 3, we plot the damping of the oscillations of the soliton parameters and compare it to the theoretical formula. In Fig. 4 the trapping of a soliton with an initial velocity is shown. The final position of the soliton is given by (22).

We have also simulated the original equation (7) with the external drive $f(\phi) = \sin(2\phi)$ and $\eta = 0.125$. We plot one of the obtained results in Fig. 5 (to be compared with Fig. 3), which shows full agreement.

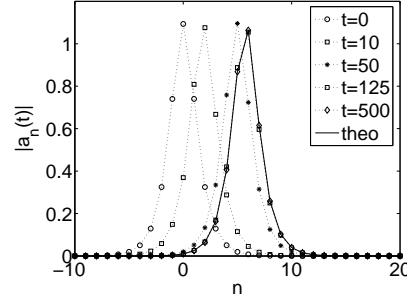


FIG. 4: Here $\gamma = 0$, $\beta = 1$, $\alpha = 0.022$, $\epsilon = 0.02$. The initial condition is a soliton with $\phi = \pi$, $x_+ = 0$, $\eta = 0.1$, and $\theta = \pi$. We plot the soliton profiles $|a_n(t)|$ at different times, which exhibits the trapping of the moving soliton. The solid line is the theoretical stable stationary soliton centered at $x_F = 5.76$ given by (22).

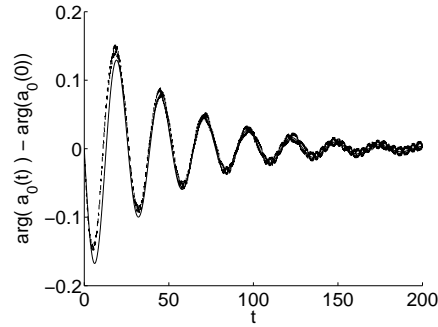


FIG. 5: Numerical simulation of Eq. (3). Here $\gamma = 0$, $\beta = 1$, $\alpha = 0.022$, $\epsilon = 0.02$, $f(\phi) = \sin(2\phi)$ and $\eta = 0.125$. The initial condition is a soliton with $\phi = \pi$, $x_+ = 0$, $\eta = 0$, and $\theta = \pi + 0.02$. We plot the phase of $a_0(t) = u_0(t) + i\sin(16t)$ (dashed line). The observed oscillations and damping are correctly predicted by the model, and correspond exactly to the ones of the solution of the averaged equation (see Fig. 3).

C. Periodic solutions of the damped AL equation with parametric drive

In the following we discuss exact periodic solutions of the parametrically damped and driven AL equation

$$iA_{nT} + [A_{n+1} - (2 + \gamma)A_n + A_{n-1}] + [i + (1 + i)\beta_n^2](A_{n+1} + A_{n-1}) = -iA_n + \overline{A_n}; \quad (23)$$

where γ models a small dispersive and nonlinear damping. To this regard we consider periodic stationary solutions of the form

$$A_n = A e^{i \ln[(n + x_F)/m]}; \quad (24)$$

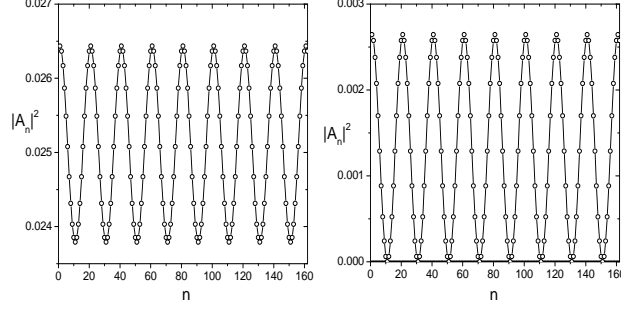


FIG. 6: Left panel: Square modulus of the dn solution in Eq. (24) with $m = 0.1$, $\phi = 0.161244$ ($N_p = 20$), $x_F = 0$, on a line of 160 points. The parameters are fixed as $\alpha = 0.04$, $\beta = 0.02$, $\gamma = 0.01558$, $\delta = 0$. Right panel: Square modulus of the cn solution in Eq. (28) with parameters fixed as in the left panel.

Direct substitution of Eq. (24) into Eq. (23) shows that a solution is indeed obtained provided the two following relations are satisfied by the soliton parameter ϕ and the modulus m :

$$2 + \frac{2 \frac{\text{dn}(\phi; m)}{\text{cn}(\phi; m)^2} + 1}{2} - \frac{2 \frac{\text{dn}(\phi; m)}{\text{cn}(\phi; m)^2}}{2} = 0; \quad (25)$$

$$N_p = 2K(m); \quad (26)$$

where N_p is the number of sites in one period and $K(m)$ is the complete elliptic integral of the first kind. Here $m \in (0; 1)$ and N_p must be a positive integer, so that there exists a numerable set of pairs $(\phi; m)$ that satisfy the conditions (25-26). If the conditions are fulfilled, then the periodic function (24) is a solution of (23) with the amplitude A and phase ϕ given by

$$A = \frac{\text{sn}(\phi; m)}{\text{cn}(\phi; m)}; \quad \phi = \frac{1}{2} \arcsin \left(\frac{2 \frac{\text{dn}(\phi; m)}{\text{cn}(\phi; m)^2}}{2} \right); \quad (27)$$

while the soliton center x_F is arbitrary.

Another periodic solution of Eq. (23) can be constructed by replacing the function dn into the ansatz (24) with the elliptic cosine cn:

$$A_n = A e^{i \phi} \text{cn}[(n + x_F); m]; \quad (28)$$

In this case the two conditions to be satisfied by ϕ and m are

$$2 + \frac{2 \frac{\text{cn}(\phi; m)}{\text{dn}(\phi; m)^2} + 1}{2} - \frac{2 \frac{\text{cn}(\phi; m)}{\text{dn}(\phi; m)^2}}{2} = 0; \quad (29)$$

$$N_p = 4K(m); \quad (30)$$

and the soliton amplitude and phase are

$$A = \frac{P}{m} \frac{\text{sn}(x; m)}{\text{dn}(x; m)}; \quad \phi = \frac{1}{2} \arcsin \frac{\text{sn}(x; m)}{\text{dn}(x; m)} + \frac{2}{\text{dn}(x; m)^2} : \quad (31)$$

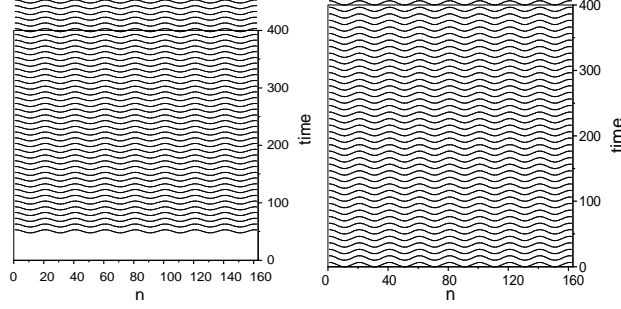


FIG. 7: Time evolution of $|A_n|^2$ for the dn (left panel) and cn (right panel) solutions in Fig. 6.

It may be worth noting that in deriving these solutions usage of the following identities for the Jacobi elliptic functions [19] have been made:

$$\text{dn}(x+a; m) + \text{dn}(x-a; m) = \frac{2\text{dn}(a; m)\text{dn}(x; m)}{\text{cn}(a; m)^2 + \text{sn}(a; m)^2\text{dn}(x; m)^2}; \quad (32)$$

$$\text{cn}(x+a; m) + \text{cn}(x-a; m) = \frac{2\text{cn}(a; m)\text{cn}(x; m)}{\text{dn}(a; m)^2 + m\text{sn}(a; m)^2\text{cn}(x; m)^2}; \quad (33)$$

Also notice that in the limit of infinite period (i.e. $m \rightarrow 1$) the above solutions both reduce to the AL soliton

$$A_n = \frac{\sinh(\eta)}{\cosh[(n+x_F)]} e^{i\phi} \quad (34)$$

with the soliton parameter satisfying

$$2 + \eta^2 - \frac{1}{2} (\eta^2 + 2 \cosh(\eta))^2 = 0:$$

Similar periodic solutions exist also for the unperturbed AL equation [20] and for generalized AL equations with arbitrarily high-order nonlinearities [21].

In Fig. 6 we depict the waveforms of the above solutions on a line of 160 points for the case $\gamma = 0.04$, $\beta = 0.02$, $\alpha = 0.01558$, $\delta = 0$, and the solution parameters are $m = 0.1$, $\eta = 2K(m)/N_p = 0.161244$, $N_p = 20$. We find, by direct numerical integrations of Eq. (23), that for small values of the damping and parametric driver amplitude these solutions remain stable under very long time evolution. This is shown in Fig. 7 where the time evolution obtained from direct numerical simulations of Eq. (23) is depicted for parameters $\gamma = 0.15$,

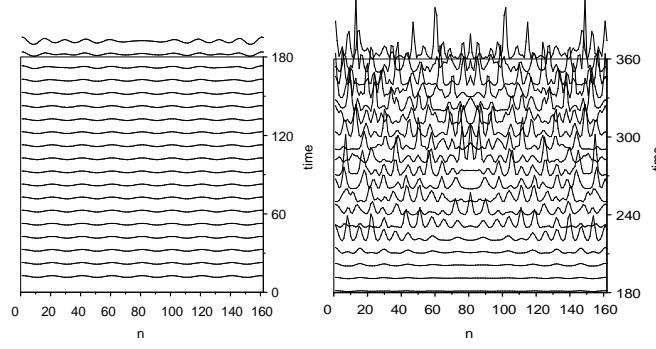


FIG. 8: Time evolution of the unstable dn solution in Eq. (24) obtained for $\gamma = 0.15$, $\beta = 0.02$, $\alpha = 0.098438$, $\delta = 0$, and the solution parameters are as in Fig. 6: $m = 0.1$, $\omega = 2K(m)N_p = 0.161244$, $N_p = 20$. Notice the change in the \mathcal{A}_n^2 scale from one panel to another.

$\gamma = 0.02$, $\beta = 0.098438$, $\delta = 0$, which supports the same dn and cn solutions as in Fig. 6. By keeping fixed the damping constant and increasing the amplitude of the parametric driver in a certain range, we find that these solutions remain stable for very long time, while outside of this range instabilities quickly develop. The development of the instability for out of range parameter is investigated in Figs. 8–9.

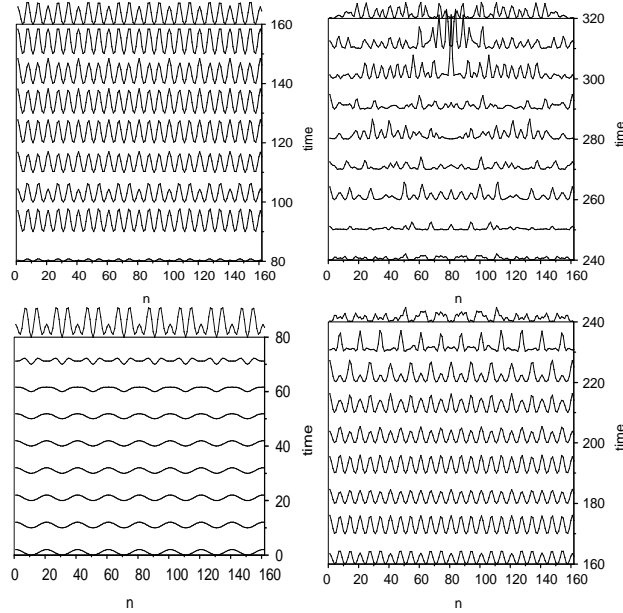


FIG. 9: Time evolution of the unstable cn solution in Eq. (28) when the parameters are fixed as in Fig. 6. Notice the change in the \mathcal{A}_n^2 scale passing from one panel to another.

Notice that while for the dn solution the instability suddenly sets in without any apparent

pattern, the instability of the cn solution seems to follow a precise pattern. In particular, from Fig. 9 we see that before the instability fully develops at time $t = 200$ the cn solution bifurcates into a period three solution at $t = 80$ which remains stable for a long time. The presence of a small dispersive nonlinear damping (controlled by the parameter γ) effectively increases the stability of both the period one and the period three solutions, as one can see from Fig. 10. The scenario behind the development of the instability of the cn solution is quite interesting and deserves more investigations.

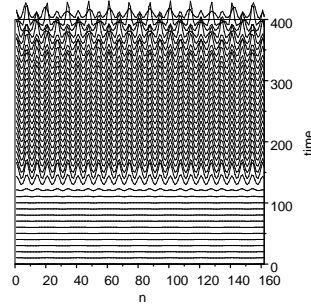


FIG. 10: Time evolution of the unstable dn solution in Eq. (24) obtained for $\gamma = 0.02$. Other parameters are fixed as in Fig. 9.

IV. THE DAMPED DNLS SYSTEM WITH PARAMETRIC DRIVE

We consider in this section that the nonlinear term is not of the AL type but it is a mixture of the AL cubic intersite nonlinearity and the onsite DNLS cubic term. We shall analyze this system by considering such a nonlinearity as a perturbation of the cubic AL nonlinearity.

A. Perturbation theory for the cubic nonlinearity

In this subsection we consider the perturbed AL equation (7) when the perturbation is given by

$$R_n = \gamma A_n^2 (A_{n+1} + A_{n-1} - 2A_n) \quad (35)$$

If $\gamma = 0$, then Eq. (7) with the perturbation (35) is the integrable AL equation. If $\gamma = 1$, then it is the standard DNLS equation. In the adiabatic approximation, this perturbation

has no effect on the first-order differential equation for the amplitude soliton parameter ϕ , but the evolution equations for the parameters x , ϕ , and η have corrective terms

$$\dot{x}_T = 2(1 - \frac{\sinh^2}{2 \cosh^2}) \sin^2 + 2 \frac{\sinh^2}{2 \cosh^2} \sin^2 \quad (36)$$

$$\dot{\phi}_T = P(x) \quad (37)$$

$$\dot{\eta}_T = 2 \cosh^2 \cos^2 + 2(1 - \cos^2) \sinh^2 \tanh^2 + 2(1 - \frac{\sinh^2}{2 \cosh^2}) \sin^2 \frac{\sinh^2}{2 \cosh^2} + 2 Q(x) \quad (38)$$

where

$$P(x) = \sum_{s=1}^X \frac{8^s s^2 \sinh^2}{3 \sinh(\frac{2s}{2})} \sin(2sx) \quad (39)$$

$$Q(x) = 1 + \frac{\sinh^2}{2} \frac{\sinh^2}{2} \sinh^2 \tanh^2 + 2 \sum_{s=1}^X \frac{2^s s^2 \sinh^2 \cosh^2 + [4s^2 \coth^2(\frac{2s}{2}) - 2^s s^2] \sinh^2}{4 \sinh(\frac{2s}{2})} \cos(2sx) \quad (40)$$

We should keep in mind that the adiabatic approximation is valid when the perturbation (35) is small, which is true if η is small and ϕ is arbitrary, or if ϕ is arbitrary and η is small. In the following, we shall only keep the terms $s = 1$ in the sums (39-40), to simplify the algebra, although the analysis could be carried out with the full expressions. This simplification is consistent with the adiabatic approximation.

B. Parametrically driven DNLS solitons

We now consider that the perturbation R_n is given by (8), that is the sum of the cubic perturbation (35) and the parametric drive with damping (9). In these conditions, there are two fixed points if $\gamma < 0$ (which is equivalent to $\gamma < 0$) and $\gamma + \eta > 0$ (which is equivalent to $\eta > 0$):

$$\eta = 0; \quad \sin(2\phi) = -\frac{\gamma}{2}; \quad \cos(2\phi) = \frac{1 - \frac{\gamma^2}{4}}{2}; \quad (41)$$

$$\cosh(\eta) = 1 + Q(0) = \frac{1}{2} + \frac{1}{2} \frac{P(\frac{\gamma}{2})}{\frac{\gamma^2}{4}}; \quad (42)$$

The center of the soliton x_m must be an integer as soon as $\gamma > 0$. This is a manifestation of the Peierls-Nabarro barrier [16, 22]. Note that the function $\eta = \cosh(\eta) = 1 + Q(0)$

is a one-to-one increasing function from $(0;1)$ to $(0;1)$ for any $\epsilon > 0$. Therefore, the parameter ϵ is uniquely determined. The picture is the same as in the perturbed AL case. The only difference is a renormalization of the amplitude parameter ϵ given by (42) instead of (15).

We next perform the linear stability analysis of the fixed points. The linearization of the system of ordinary differential equations for the soliton parameters around the stationary points gives:

$$\dot{\epsilon}_T = -4 \tanh \epsilon \cos(2\epsilon) \epsilon_1; \quad (43)$$

$$\dot{\epsilon}_T = -2 \epsilon_1 + 16 \epsilon^4 \frac{\sinh^2 \epsilon}{3 \sinh(\frac{\epsilon}{2})} x_1; \quad (44)$$

$$\dot{\epsilon}_T = 2 [\sinh \epsilon + \epsilon Q(\epsilon)] \epsilon_1 - 2 \epsilon_1; \quad (45)$$

$$x_{1T} = 2(1 - \frac{\sinh \epsilon}{2}) \epsilon_1 + 2 \frac{\sinh^2 \epsilon}{2 \cosh \epsilon} \epsilon_1 - \frac{\tanh \epsilon}{3} \frac{\epsilon^2 + 4 \epsilon^2}{6} \cos(2\epsilon) \epsilon_1 - \frac{\tanh \epsilon}{2} \frac{4 \epsilon^2}{\sinh(\frac{\epsilon}{2})} x_1; \quad (46)$$

This 4 × 4 linear system can be decomposed into two 2 × 2 linear systems, for $(\epsilon_1; \epsilon_1)$ and for $(\epsilon_1; x_1)$, respectively. It is then easy to compute the eigenvalues. They are:

$$\begin{aligned} \lambda^{(1)} &= -4 \tanh \epsilon \cos(2\epsilon); \\ \lambda^{(2)} &= -2; \\ \lambda^{(3)} &= 1 + \frac{\tanh \epsilon}{2} \frac{\epsilon^2}{\sinh(\frac{\epsilon}{2})} + \tilde{\lambda}; \\ \lambda^{(4)} &= 1 + \frac{\tanh \epsilon}{2} \frac{\epsilon^2}{\sinh(\frac{\epsilon}{2})} + \tilde{\lambda}; \end{aligned}$$

where the complex numbers $\tilde{\lambda}$ and $\tilde{\lambda}^*$ are given by

$$\tilde{\lambda}^2 = -2 \epsilon^4 \tanh \epsilon \cos(2\epsilon) [\sinh \epsilon + \epsilon Q(\epsilon)] \epsilon_1; \quad (47)$$

$$\begin{aligned} \tilde{\lambda}^2 &= -2 \epsilon_1 \frac{\tanh \epsilon}{2} \frac{\epsilon^2}{\sinh(\frac{\epsilon}{2})} \\ &+ 16 \epsilon^4 \frac{\sinh^2 \epsilon}{3 \sinh(\frac{\epsilon}{2})} - 2(1 - \frac{\sinh \epsilon}{2}) \epsilon_1 + 2 \frac{\sinh^2 \epsilon}{2 \cosh \epsilon} \\ &\quad - \frac{\tanh \epsilon}{3} \frac{\epsilon^2 + 4 \epsilon^2}{6} \cos(2\epsilon) \epsilon_1 \end{aligned} \quad (48)$$

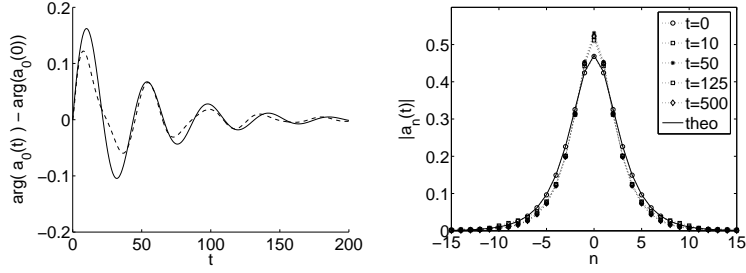


FIG. 11: Here $\beta = 1$, $\gamma = 0.3$, $\epsilon = 0.022$, $\delta = 0.02$. The T and t scales coincide. The initial condition is a soliton with $\eta = \eta_+$, $x_+ = 0$, $v = 0$, and $\phi = \eta_+ 0.02 = 0.43$. We plot in the left picture the argument of $a_0(t)$ (dashed line). The observed oscillations and damping are correctly predicted by the model. The period is $2\pi\omega_+ = 43.9$ and the exponential decay rate is $\gamma = 0.02$ (solid line). Note also, in the right picture, that the stationary profile is not exactly the sech predicted by the AL theory, but a slightly deformed version.

The eigenvalues $\lambda^{(1)}$ and $\lambda^{(2)}$ describe the growth rates of the perturbations of the amplitude parameter η and phase parameter ϕ . The eigenvalues $\lambda^{(3)}$ and $\lambda^{(4)}$ describe the growth rates of the perturbations of the velocity parameter v and soliton center x .

The function $\gamma \sinh(\eta) + \epsilon Q(0)$ is positive valued. Therefore the real part of the eigenvalue $\lambda^{(1)}$ is positive and the stationary point labelled η_+ is unstable. Besides, the real parts of the eigenvalues $\lambda_+^{(1)}$ and $\lambda_+^{(2)}$ are non-positive for any $\eta_+ > 0$. The real parts of $\lambda_+^{(3)}$ and $\lambda_+^{(4)}$ are also non-positive, which implies that the stationary point labelled η_+ is stable.

When η_+ is large (say equal to 1), it is important to choose a suitable value γ so that the soliton parameter η_+ defined by (42) is small (more exactly, smaller than 0.5). Indeed, the theoretical analysis based on the perturbed IST is valid only in this case. Furthermore, numerical simulations show that (42) is not a stationary point for larger values of η_+ , which shows the fundamental limitation in the perturbed IST. Within this region of parameters, the soliton parameters η and ϕ oscillate with the frequency ω_+ given by (47) and they also experience an exponential decay with the rate γ . The oscillation period and damping rate are confirmed by numerical simulations (Fig. 11).

Moreover, as in the AL case, the propagation of moving solitons is not supported, as the soliton velocity decays exponentially to 0. If we denote by η_0 the initial value of the parameter η , then the input soliton converges to its stationary form centered at

$$x_F = (1 - \frac{\sinh \eta_+ + \sin \eta_0}{\cosh \eta_+}) \frac{\sinh^2 \eta_+ + \sin \eta_0}{\cosh \eta_+} : \quad (49)$$

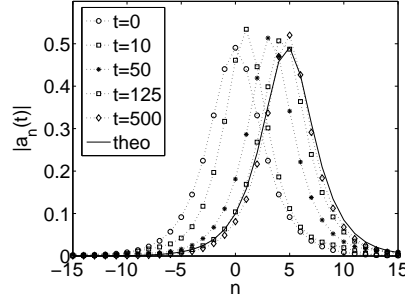


FIG. 12: Here $\gamma = 1$, $\beta = 0.3$, $\alpha = 0.022$, $\epsilon = 0.02$. The initial condition is a soliton with $a_0 = 1$, $x_+ = 0$, $\phi = 0.1$, and $\theta = \pi = 0.45$. We plot the soliton profiles $|a_n(t)|$ at different times, which exhibits the trapping of the moving soliton. The solid line is the theoretical stable stationary soliton centered at $x_F = 4.82$ given by (49).

Notice that we have neglected higher-order term (in ϵ) in this expression, which is consistent with the previous hypotheses and which gives a very accurate prediction for the final soliton position (see Fig. 12).

V. CONCLUSION

In this paper we have investigated the existence and stability properties of new types of bright discrete solitons in discrete nonlinear Schrödinger-type models with damping and strong rapid drive. Stable stationary solitons are exhibited in the case of a general cubic nonlinearity. If the nonlinearity has the special AL form, then stationary solitons, moving solitons, and periodic trains of solitons are found to be stable solutions of the system. These results have been obtained by applying a perturbed inverse scattering transform to the averaged equation and confirmed by numerical simulations. This means that the inverse scattering theory is useful for probing the parameter space and exhibiting interesting phenomena. One of the problems that should be addressed for future consideration is the mechanisms responsible for the instabilities of the periodic cn and dn solutions for large drive, which seem to be different since a chaotic instability appears first in the dn case, while new patterns with different periods appear in the cn case.

[1] M. J. Ablowitz and Z. H. Musslimani, Phys. Rev. Lett. 87, 254102 (2001).

- [2] A . Trombettoni and A . Smerzi, Phys. Rev. Lett. 86, 2353 (2001); F . K h . Abdullaev, B . B . Baizakov, S . A . Darm anyan, V . V . K onotop, and M . Salemo, Phys. Rev. A 64, 043606 (2001).
- [3] F . K h . Abdullaev, E . N . T soy, B . A . M alomed, and R . A . K raenkel, Phys. Rev. A 68, 053606 (2003).
- [4] A . V . Ustinov, C . Coqui, A . Kemp, Y . Zolotaryuk, and M . Salemo, Phys. Rev. Lett. 93, 087001 (2004).
- [5] D . N . Christodoulides and N . Efremidis, Opt. Lett. 27, 568 (2002).
- [6] G . J . de Valcarcel and K . Staliunas, Phys. Rev. E 67, 026604 (2003).
- [7] U . Peschel, O . Egorov, and F . Lederer, Opt. Lett. 29, 1909 (2004).
- [8] A . V . Gorbach, S . Denisov, and S . Flach, Opt. Lett. 31, 1702 (2006).
- [9] M . Kollmann, H . W . Capel, and T . Bountis, Phys. Rev. E 60, 001195 (1999).
- [10] D . Hennig, Phys. Rev. E 59, 001637 (1999).
- [11] H . Susanto, Q . E . Hoq, and P . G . Kevrekidis, arXiv:1106.05007.
- [12] I . V . Barashenkov, M . M . Bogdan, and V . I . K orobov, Europhys. Lett. 15, 113 (1991).
- [13] V . V . Alexeeva, I . V . Barashenkov, and D . E . Pelinovsky, Nonlinearity 12, 103 (1999).
- [14] M . Salemo, Phys. Rev. A 46, 6856 (1992).
- [15] N . K . Efremidis and D . N . Christodoulides, Phys. Rev. E 67, 026606 (2003).
- [16] A . A . Vakhnenko and Yu . B . Gaididei, Teor. Mat. Fiz. 68, 350 (1986) [Theor. Math. Phys. 68, 873 (1987)].
- [17] D . Cai, A . R . Bishop, and N . Gronbech-Jensen, Phys. Rev. E 53, 4131 (1996).
- [18] E . V . Doktorov, N . P . Matsuka and V . M . Rothos, Phys. Rev. E 68, 066610 (2003).
- [19] A . K hare and U . Sukhatm e, J. Math. Phys. 43, 3798 (2002); A . K hare, A . Lakshminarayan, and U . Sukhatm e, J. Math. Phys. 44, 1822 (2003); J. Phys. 62, 1201 (2004).
- [20] R . Scharf and A . R . Bishop, Phys. Rev. A 43, 6535 (1991).
- [21] A . K hare, K . Rasmussen, M . Salemo, M . R . Samuelsen, and A . Saxena, Phys. Rev. E 74, 016607 (2006).
- [22] O . O . Vakhnenko and V . O . Vakhnenko, Phys. Lett. A 196, 307 (1995).